Road Snow Coverage Estimation Using Camera and Weather Infrastructure Sensor Inputs

Parth Kadav Western Michigan University

Nicholas A Goberville Argonne National Laboratory

Kyle Prins Western Michigan University

Amanda Siems-Anderson and Curtis Walker National Center for Atmospheric Research

Farhang Motallebiaraghi, Kyle Carow, Johan Fanas Rojas, Guan Yue Hong, and Zachary Asher
Western Michigan University

Abstract

Modern vehicles use automated driving assistance systems (ADAS) products to automate certain aspects of driving, which improves operational safety. In the U.S. in 2020, 38,824 fatalities occurred due to automotive accidents, and typically about 25% of these are associated with inclement weather. ADAS features have been shown to reduce potential collisions by up to 21%, thus reducing overall accidents. But ADAS typically utilize camera sensors that rely on lane visibility and the absence of obstructions in order to function, rendering them ineffective in inclement weather. To address this research gap, we propose a new technique to estimate snow coverage so that existing and new ADAS features can be used during inclement weather. In this study, we use a single camera sensor and historical weather data to estimate snow coverage on the road. Camera data was collected over 6 miles of arterial roadways in Kalamazoo, MI. Additionally, infrastructure-based weather sensor visibility data from an Automated Surface Observing System (ASOS) station was collected. Supervised Machine Learning (ML) models were developed to determine the categories of snow coverage using different features from the images and ASOS data. The output from the best-performing model resulted in an accuracy of 98.8% for categorizing the instances as either none, standard, or heavy snow coverage. These categories are essential for the future development of ADAS products designed to detect drivable regions in varying degrees of snow coverage such as clear weather (the none condition) and our ongoing work in tire track detection (the standard category). Overall this research demonstrates that purpose-built computer vision algorithms are capable of enabling ADAS to function in inclement weather, widening their operational design domain (ODD) and thus lowering the annual weather-related fatalities.

Introduction

According to the Fatality Analysis Reporting System (FARS) encyclopedia by the National Highway Traffic Safety Administration (NHTSA), there were nearly 103,172 fatal crashes from the year 2018-2020 in the United States [1]. Out of these fatal crashes, nearly 10% were related to inclement weather such as snow, ice, sleet, and rain. Similarly, during 2007-2016, weather-related vehicular crashes accounted for nearly 21% of all reported crashes annually resulting in 16% of crash fatalities and 19% of crash injuries throughout the United States [2]. It is really crucial to understand how different weather conditions can affect the transportation network. Fundamentally, adverse weather conditions can cause 1) Impairment of situational awareness and 2) Inhibitions to vehicular maneuverability [3]. Due to poor visibility caused by heavy rain, blowing dust or snow, or dense fog, multi-vehicle collisions can occur when drivers lose awareness of their position, location, and speed in relation to other cars. Automated vehicles can open the way for dependable and safe driving in any weather [4]–[7].

Nearly 94% to 96% of all auto accidents are caused due to human errors (speeding, aggressive/reckless driving, distracted driving, chemical impairment, and drowsy driving), which are preventable according to a study conducted by NHTSA in 2016 [8]. ADAS systems were created to automate driving tasks, improve aspects of the driving experience, and

increase safety and safe driving practices [9]. About 40% of all accidents in passenger vehicles can be prevented or significantly reduced with the use of ADAS features including Forward Collision Warning (FCW), Automated Emergency Braking (AEB), Lane Departure Warning (LDW), Lane Keeping Assistance (LKA), blind spot warning assistance, and many more. [4, 10]–[12]. Furthermore, ADAS features such as FCW and AEB alone reduce front-to-rear crashes by nearly 50% [6]. From the 1,853 driver injury crashes studied in [13, 14], it was discovered that LDW and LKA systems were able to reduce head-on and single-vehicle crashes on roads at higher speed limits (45-75 mph) and visible lane markings by nearly 53%. Based on the statistics, ADAS features such as LDW, LKA, AEB, and FCW significantly cut down on collisions caused by human and external variables [15].

One of the ways that ADAS improves safety is to provide vital information about the vehicle and its surroundings by classifying road lanes [16, 17]. Lane recognition is the foundation of many driving assistance systems such as LKA, LDW, and Lane Centering Assist (LCA), specifically identifying lane markings. During snowy conditions, lane markings can get obscured or hidden which can render driving assistance systems ineffective. In reality, snow accumulation on highways frequently leads drivers to disregard lane positions and drive on different regions of the road as necessary, in other words, forming informal auxiliary traffic lanes [3]. The poor performance of driver assistance systems in adverse weather conditions, such as rain, snow, fog, and hail, is among the most crucial challenges in vehicle automation. Unfortunately, just like a human's vision, the sensors used by driving assistance systems can be negatively affected by inclement weather. Rainy and foggy conditions cause significant degradation in the performance of Camera, Radar, and LiDAR [18, 19]. The LiDAR will misdetect objects under rainy and snowy conditions due to rain droplets, snow particles, and ice [20]. Similarly, Radar, which is used for many driver assistance systems such as adaptive cruise control (ACC) and AEB, has an issue with signal attenuation in the rain [18, 21, 22]. On-board vehicle cameras are essential in providing both the systems and the driver with crucial information. Cameras come standard in all vehicles with level 1 and level 2 autonomy [23]. Various sensors operate differently in various weather conditions, according to the literature review conducted in this section. To enable ADAS performance in inclement weather conditions and actively toggle between sensors based on environmental conditions, a method to determine the category of road conditions in inclement weather needs to be established so that purpose-built perception techniques can be deployed.

There are few studies in the literature that address the issue of estimating road weather conditions for inclement weather. One such study conducted in 2011 introduced a method of estimating road weather using a ML model trained with camera images and Road Weather Information Systems (RWIS) data [24, 25]. The results from this study indicate that the model was capable of achieving a 91% accuracy on the test set for classifying the road conditions into five different categories (dry, ice, snow, track and wet). This study utilized Principal Component Analysis (PCA) to determine which inputs contributed the greatest to model performance.

The model used limited training data and had a biased dataset gathered from static images at intersections. Another study conducted by Qian proposes a system that categorizes road conditions using static images using a camera [26]. This study obtained an accuracy of 68% on classifying the road conditions into dry, wet, and snow. However, this study only uses a dataset of 100 images with a 50-50 train test split. Having such a small dataset, specifically a small training set can lead to poor performance and generalization. The methods and results of these studies provide ways to estimate the weather conditions mainly for object-dependent ADAS purposes and do not talk about lane-dependent features such as lane lines, road type, and amount of snow coverage in the lane which are independent of any objects in the environment. Additionally, they only employ camera data using a small dataset as the input, and no additional input is provided to the models. Therefore, a more rigorous study of snow coverage estimation using a multi-input model is needed to move this research forward. It is crucial for estimating the road snow coverage in order to expand the ODD of ADAS and use algorithms that detect the drivable region in snow-occluded lane lines as done in our previous studies [12, 27].

To address the need for real-time estimation of road snow coverage, the proposed method uses Machine Learning (ML) models that use camera data and infrastructure weather sensor data as inputs to predict road snow coverage. We recorded and labeled each image in different categories based on the subjective level of snow coverage on the road. The three different snow coverage categories were none, standard and heavy. The images were processed using feature engineering, and different image features were obtained. The inputs to the ML models were the image-level features and ASOS infrastructure weather sensor features. We tested the performance of the different models on key metrics such as accuracy, precision, recall, and F1 score. The goal of this work is to provide a robust snow coverage estimation method for ADAS perception systems using a single-camera sensor and infrastructure-based weather sensor data. The methods discussed in the next section talk about the details of the different feature sets, ML methods, and the overall performance of the various models in classifying road snow coverage.

Methodology

In this section, we will first examine the drive cycle that was selected, the vehicle platform, and the equipment used, followed by a discussion of the methods to collect and prepare the data. Following that, several ML models will be developed and assessed.

Drive Cycle

The drive cycle consisted of the two-lane arterial roads in Kalamazoo, MI. The route was selected based on having low traffic volume, two lanes, clear visible lane lines, and occluded lane lines. Arterial roads receive snow level variation as they are plowed irregularly and have a low amount of traffic which results in varying amounts of snow coverage. The route

FIGURE 1   Road segments used for data collection during the winter of 2020-2021 in Kalamazoo, MI.
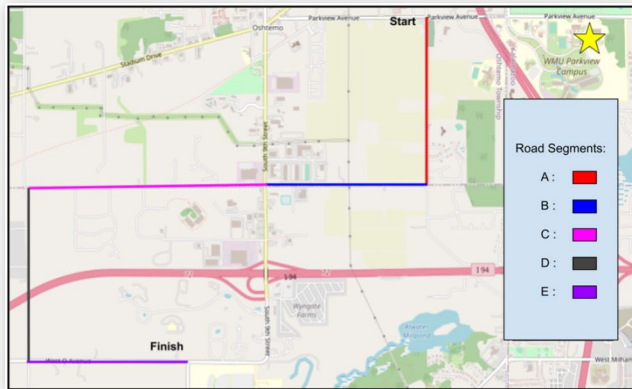
consisted of 5 different road sections, which were A, B, C, D, and E each one mile in length with different cardinal directions. To add variation to the dataset, the data was collected on different days with changing snow precipitation forecast through the 5 different road segments during the winter of 2020-2021.

Vehicle Platform and Sensors

The Energy Efficient Autonomous Vehicles (EEAV) research vehicle platform, shown in Figure 2, was used to collect data. This is a 2019 Kia Niro and includes a forward-facing RGB camera, Polysync Drivekit, Neousys in-vehicle computer, vehicle Controller Area Network (CAN) bus interface, and a Mobileye camera. We used the forward-facing ZED 2 RGB camera from Stereolabs [28]. The ZED 2 is a widely available machine vision camera, which is available with a Software Development Kit (SDK) that provides greater functionality for our instrumented research vehicle. The ZED 2 provided us with the raw RGB images used to build the dataset. We have used the ZED 2 along with its SDK for our previous studies, but potentially any RGB camera could be used for this study [10, 12]. The images were captured at a resolution of 1280 x 720 and at a frame rate of 30 frames per second

Infrastructure Weather Sensor

This study used historical weather data collected by the Automated Surface Observation System or ASOS station located at the Kalamazoo Battle Creek International Airport.

FIGURE 2   (a) Kia Niro Instrumented Research Vehicle, (b) ZED 2 stereo camera.

ASOS is considered a "gold standard" observation, used widely in the atmospheric sciences [29]. The intention of ASOS was to provide reliable and useful automated weather observations in a cost-effective manner [30]. The ASOS dataset used contains weather data observations for the corresponding days of collected drive cycles. This data is published in one-minute intervals for parameters such as visibility, temperature, wind characterization, precipitation, and atmospheric pressure. While ASOS stations are capable of observing falling precipitation, there are a number of issues that can lead to erroneous precipitation reports. These include the inability to recognize precipitation type for frozen or mixed precipitation events [31] and undercatch of snowfall amount or intensity in strong winds [32]. However, in the U.S., snowfall intensity is measured not by accumulation but by visibility, with light snow categorized as >1 km visibility, moderate between 0.5 and 1 km visibility, and heavy snow less than 0.5 km visibility [33]. In order to calculate visibility, ASOS uses a sensor that gauges the air's clarity directly at the sensor in a condensed area. The visibility coefficient is derived based on the maximum distance the sensor can see. Due to the more reliable automated visibility observations, for this study, we focused on the visibility coefficient. The visibility coefficient only serves as an additional input to the ML models and we are not interested in finding the relation between the raw dataset and the visibility coefficient.

Data Pipeline

Figure 3 shows the overall model development pipeline. This pipeline shows the different steps taken to achieve model results.

Data Selection and Filtering

We collected ~ 100,000 RGB images. The images were resampled from 30 fps to match the ASOS dataset. As the ASOS data was sampled every minute (0.167 Hz), we had to map the images with ASOS data based on the timesteps. Further quality control was taken into account and these images were assessed for poor quality such as over-exposed images from sun glare, windshield wiper obstruction, image noise, distortion, etc. When finished the final dataset had a total of 20,883 images spanning across the five road sections on different days.

FIGURE 3   Overall model development pipeline.
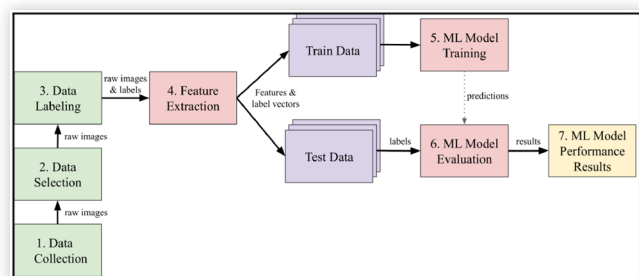
Labeling

A subjective method was used to place data from each road segment into three categories: none, standard, or heavy. We had collected the dataset and visually assessed each image for snow coverage. After looking at the entire dataset, we could find that all road segments fell into three main categories. Each of the road segments were assigned into one of these categories based on how much snow was covering the surface of the road. Figure 4 shows the three different snow conditions. Figure 4a shows the none condition, Figure 4b shows the standard condition, and Figure 4c shows the heavy condition. We labeled all the images in the dataset based on the subjective snow condition.

Feature Extraction

To build and train the ML models, we first needed to preprocess the data and then extract features. Feature extraction transforms raw data into numerical features the model can process while retaining original data. This works better than applying ML to the raw dataset [34]. To start the process of feature engineering, the raw image was first resized to 256 x 256 from its original dimensions of 720 x 1280. Resizing results in reduced computational load while training models. To further improve feature detection and reduce computational complexity, images were masked with a static Region of Interest (ROI) that only included the road surface as shown in Figure 5. The Road ROI mask (Figure 5b) was then fused with the raw image (Figure 5a) to output the Masked ROI (Figure 5c). The masked ROI contains less than 10% of the total pixels when compared to the raw image. Similar to our previous study, we decided to create different feature sets, each containing various image features, which will help in identifying features that perform better compared to others. [10]

Images contain pixel-level color channel values which are contained in 3 dimensional arrays which contain the Red, Green and Blue values for each pixel (RGB). For this study we decided to use the RGB mean and standard deviation
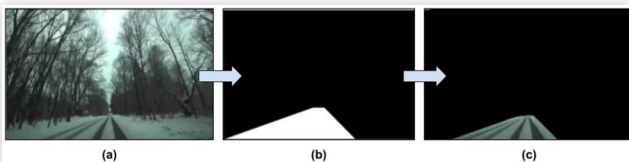
values as the image-level features. The RGB values change as the level of snow coverage changes in the image, with a lower road snow coverage, we have lower overall RGB intensities in the image and as the snow coverage increases the RGB intensities increase. These features strongly correlate with the changing snow coverage on the road.

Table 1 shows the different feature sets that were created for this study. We organized these features into sets where each set has its corresponding feature vector. For example, feature set 0 has three feature vectors which are the mean values for the red, green and blue color channels in the masked ROI image, feature set 2 has six feature vectors which are the mean (Equation 1) and standard deviation (std. dev) (Equation 2)

$$\bar{x} = \frac{1}{N}\sum_{i=1}^{N} x_i \qquad \text{(Eq.1)}$$

$$\sigma = \sqrt{\frac{\sum(x_i - \mu)^2}{N}} \qquad \text{(Eq. 2)}$$

values for red, green and blue color channels respectively. Feature set 3,4 and 5 include the ASOS visibility coefficient input along with the image-level features. Each feature set has its own feature array X, the shape of feature array $X = (m \times n)$ dimensions where m = number of images in the array and n = number of features. The feature array X is the input. Similarly label vector $y = (m \times 1)$ dimensions, where m is the number of images in array corresponding to the feature array X representing the subjective snow coverage, as mentioned in the labeling location section (*none* : 0, *standard* : 1, *heavy* : 2). Each element in the label vector maps the label to its corresponding input from the feature array X. The dataset was split into 70 - 30% for training and testing.

TABLE 1 Included feature sets used in model development along with their array shapes.

Feature Set	Included Feature Vector	Train Array Shape (m = 14,618)	Test Array Shape (m = 6265)
0 (Img-level)	R,G,B (mean)	(14,618, 3)	(6,265, 3)
1 (Img-level)	R,G,B (std. dev)	(14,618, 3)	(6,265, 3)
2 (Img-level)	R,G,B (mean), R,G,B (std. dev)	(14,618, 6)	(6,265, 6)
3 (Img-level + ASOS)	R,G,B (mean), visibility coefficient	(14,618, 4)	(6,265, 4)
4 (Img-level + ASOS)	R,G,B (std dev), visibility coefficient	(14,618, 4)	(6,265, 4)
5 (Img-level + ASOS)	R,G,B (mean), R,G,B (std. dev), visibility coefficient	(14,618, 7)	(6,265, 7)

FIGURE 4   (a) none condition, (b) standard condition, and (c) heavy condition.

FIGURE 5   (a) Raw Image, (b) ROI, and (c) Masked ROI.

Machine Learning Techniques

We evaluated different types of ML algorithms to test which models perform better in combination with the different types of feature sets. The six different ML models that were evaluated were: Decision Trees (dtrees), Random Forests (rforest), K-Nearest Neighbors (KNN), Logistic Regression, Support Vector Machines (SVM), and Naive-Bayes (naive). These models were selected based on their capabilities and demonstrated performance for computing classification tasks for computer vision applications. [35]–[37].

Let us look at an overview of all the models used in this study and their computational capabilities. Dtrees and rforest work by making a series of logical decisions mapped as nodes on a tree. This offers insight into relevant features. Training these models is computationally heavy. Both decision trees and random forest work well with less number of features. Logistic Regression works by fitting a logistic curve to the data and works well on datasets in which there is minimal overlap on the classes. Naïve Bayes offers a relatively simple model and performs well on datasets with less features that are independent of each other. Support Vector machines work by mapping the data points onto a space with more than two dimensions and then finding a hyperplane that groups them. K Nearest Neighbors is a simple algorithm that performs well in classification tasks. With our dataset k neighbors are used to label new data based on proximity to neighboring datapoint. KNN works well with large, noisy datasets. [38, 39]. The work in this paper was performed in Python using models provided by the open-sourced "scikit-learn" python package [40]

Evaluation Metrics

The predicted outputs of the model y_{pred} were compared with the ground truth labels y and then evaluated for various metrics. The metrics used for evaluation were prediction accuracy, precision, recall, F1 score, and average model compute time. Equations 3 to 6 show how these metrics are calculated using the four corners of the confusion matrix as shown below:

- True Positive (TP) : no. of images classified correctly with respect to their snow coverage label

- False Positive (FP) : no. of images classified incorrectly with respect to their snow coverage label

- True Negative (TN) : no. of images classified correctly with respect to a negative label

- False Negative (FN) : no. of images classified incorrectly with respect to a negative label

TP, FP, TN, and FN provide us with the different combinations of predicted and actual values which are useful to calculate crucial performance evaluation metrics such as Accuracy, Precision, Recall and F1 Score. These Accuracy is the fraction of predictions the model got right which means the number of images were correctly classified as none, standard or heavy snow based on their condition. Precision measures the quality of a model's positive prediction. Recall

displays the proportion of accurate positive predictions made among all possible positive predictions. Precision and recall together make up the F1 score.

$$Accuracy = \frac{TP + TN}{TP + TN + FP + FN} \qquad \text{Eq. (3)}$$

$$Precision = \frac{TP}{TP + FP} \qquad \text{Eq. (4)}$$

$$Recall = \frac{TP}{TP + FN} \qquad \text{Eq. (5)}$$

$$F1\ Score = 2^* \frac{precision^* recall}{precision + recall} \qquad \text{Eq. (6)}$$

Results

The results of this research include an overview of the analyses conducted for image level features and ASOS weather data features as well as the results from the ML training for estimating the snow coverage using different features as inputs. Results were obtained for a total of 35 different ML models. When using only image-level features, the order of the best-performing ML models was: SVM, Naive-Bayes, Logistic Regression, KNN, Random Forests, and Decision Trees. When we use variation in the feature sets as input to the model, such as feature set 5 which includes all image-level features and the snow visibility, we obtained the best-performing model. The results indicate that using image-level features along with the visibility coefficient from the ASOS dataset improves the performance of the model in key metrics such as accuracy, F1 score, and precision by a significant margin irrespective of the model used. To look at one such example, Figure 6 highlights the most important feature in feature set 5 for dtrees. The feature importance technique rates the input features

FIGURE 6 Feature importance for Dtrees with the feature set 5.
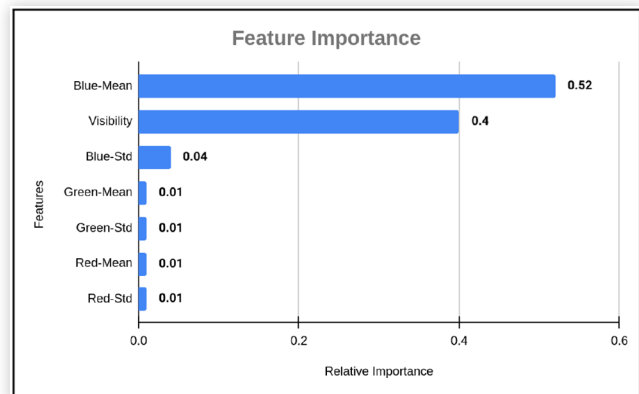
according to how well they can predict the target variable. We used skicit learn's Plot Feature Importance method to get the feature importance. The two most important features for this model and feature set combination are the blue mean value from the image-level feature and the visibility coefficient from the ASOS dataset. This implies that both image-level features and infrastructure weather sensor data input play an important role in enhancing the models performance which is consistent with the results from other models as well. (Table 2 in the appendix for all results).

To further illustrate the importance of adding the weather sensor data as an input, we obtained the confusion matrix for dtrees with all image-level features (feature set 2) in Figure 7b, and all image-level and infrastructure weather sensor data (feature set 5) in Figure 7a. The vertical axis shows the true labels and the horizontal axis shows the predicted classes. The diagonal shows the classifications for each of the snow coverage conditions as the first element in the diagonal shows the True Positives for class 0 (none), class 1 (standard), and class 2 (heavy). The confusion matrix heatmap shows that feature set 5 outputs more TP's for each class than the feature set 2.

Figure 7 shows the comparison between the 6 different models for feature set 2 and feature set 5. As seen in Figure 8 all of the models perform at least ~67% better with both image-level and weather data features (feature set 5) when compared to only image-level features (feature set 2). The best performing model for feature set 2 was svm which tied with logistic regression, and naive. Dtrees with feature set 2 performed poorly when compared to the other models. Contrastingly, adding the snow visibility input from ASOS improved the model performance significantly for all models which is shown by the blue bars. The best performing model for feature set 5 is dtrees.

Figure 9 shows Accuracy, and F1 Score by the models using all features (feature set 5). Dtrees achieved an average compute time of 9.51 seconds and rforest achieved an average compute time of 0.09 seconds. For feature set 5 the best performing models are random forest and decision trees both achieving 98.8 % Accuracy and 98.8% F1 score. As the number of features increase, both rforest and dtrees perform significantly better on the same dataset.

Some feature set combinations perform better when compared to their individual feature sets. For example, as
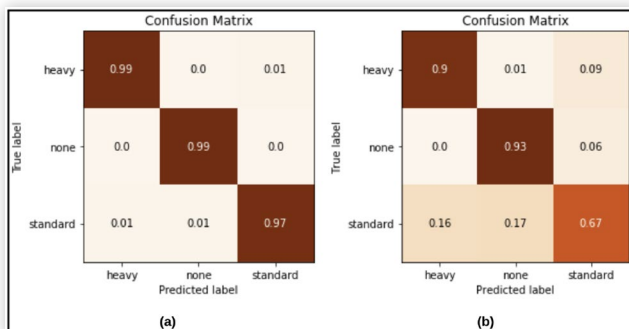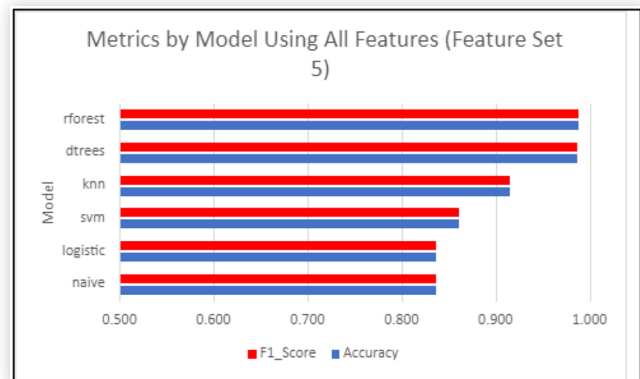
FIGURE 8   Feature Set Accuracy Comparison between feature set 2 (Image data alone) and feature set 5 (Image and Weather Data).

FIGURE 9   Comparison of Accuracy, Precision, Recall, and F1 score by model for feature set 5.

shown in Table 2 (Appendix), feature set 1 and feature set 2 yield similar results in key metrics such as accuracy, precision, recall and F1 Score. When we add weather data inputs to feature set 1 and 2, they make feature sets 3 and 4. We can observe that adding the weather data inputs significantly improved the performance of feature set 4 (originally feature set 2) when compared to the performance of feature set 3 (originally feature set 1). This shows that feature set 4 (RGB std. dev + weather data) outperformed feature set 3 (RGB mean + weather data). This implies that RGB std. dev is a better feature when compared to RGB mean in the context of our study.

So to summarise the results, both the image-level features and weather sensor input are equally important as shown in Figure 6,7,8, and 9. A critical advantage of the image data is that is that it is precisely local to the car, although the weather sensor provides excellent area-wide information that may impact road visibility, the image data from the vehicle can be used to accurately determine, with input from the general weather data, what the road conditions are in the current location of the vehicle. Adding easily available weather data from existing infrastructure is a highly effective means of improving our ability to estimate local road conditions.

FIGURE 7   Confusion matrix heat map for (a) Dtrees with feature set 5, and (b) Dtrees with feature set 2.

Conclusions

In this study we derived a method of estimating the snow coverage on the road using a single camera sensor and infrastructure weather data inputs using ML. Firstly, data was collected using the instrumented research vehicle along arterial roads in Kalamazoo, MI. This data was then processed and cleaned for model development. Additionally, infrastructure based weather sensor data such as snow visibility was acquired from ASOS. Features were extracted from the processed camera data and ASOS dataset to further create different features sets. These feature sets were used as inputs to the different supervised ML models. In total we had 35 different model-feature sets combinations. We compared and analyzed the performance of all models based on metrics such as Accuracy, Precision, Recall, and F1 score. The best-performing model using all image-level features (feature set 2) yielded an accuracy of 52.8% whereas the best-performing model with both image-level features and weather data feature (feature set 5) had an accuracy of 98.8%. This demonstrates that both image-level features and weather sensor inputs equally improve the performance of the models.

Overall this study demonstrates that we can estimate the snow coverage on the roads using a custom dataset with just one camera sensor and infrastructure weather data. Categorizing snow coverage will enable ADAS products to operate in inclement weather conditions. This study lays the foundation for broadening the ODD of AVs which will also positively impact the operation of AVs, minimizing crash injuries and fatalities. Additionally, higher resolution on-vehicle weather sensor data as inputs in conjunction with image data would further enhance the model's performance. We could get accurate local weather information from an on-vehicle weather sensor such as the MARWIS which provides us with dynamic road condition information [41]. Adding additional features available in the ASOS dataset along with the on-vehicle weather sensor data such as friction, ice percent, road condition, water film height, and precipitation would help in improving the model's performance. Future work for this study will include estimating snow coverage using data from both infrastructure and on-vehicle sensor data and using DL models.

References

1. "People - All Victims," https://www-fars.nhtsa.dot.gov/People/PeopleAllVictims.aspx (accessed Sep. 28, 2022).

2. "How Do Weather Events Impact Roads?," https://ops.fhwa.dot.gov/weather/q1_roadimpact.htm (accessed Oct. 08, 2022).

3. Neumeister, D.M. and Pape, D.B., and Battelle Memorial Institute, "Automated Vehicles and Adverse Weather: Final Report," Department of Transportation, Intelligent Transportation Systems Joint Program Office, United States, FHWA-JPO-19-755, Jun. 2019. [Online]. Available: https://rosap.ntl.bts.gov/view/dot/43772 (accessed: Oct. 01, 2022)

4. Svancara, A.M., Horrey, W.J., Tefft, B., and Benson, A., "Potential Reduction in Crashes, Injuries and Deaths from Large-Scale Deployment of Advanced Driver Assistance Systems," *AAA Foundation for Traffic Safety*, Sep. 2018. [Online]. Available: https://aaafoundation.org/wp-content/uploads/2018/09/18-0567_AAAFTS-ADAS-Potential-Benefits-Brief_v2.pdf (accessed Feb. 04, 2021).

5. Jiménez, F., Naranjo, J.E., Anaya, J.J., García, F. et al., "Advanced Driver Assistance System for Road Environments to Improve Safety and Efficiency," *Transportation Research Procedia* 14 (Jan. 2016): 2245-2254.

6. "Real-World Benefits of Crash Avoidance Technologies," Insurance Institute for Highway Safety & Highway Loss Data Institute, Dec. 2020. [Online]. Available: https://www.iihs.org/media/259e5bbd-f859-42a7-bd54-3888f7a2d3ef/shuYZQ/Topics/ADVANCED%20DRIVER%20ASSISTANCE/IIHS-real-world-CA-benefits.pdf, https://www.iihs.org/topics/advanced-driver-assistance.

7. Walker, C.L., Boyce, B., Albrecht, C.P., and Siems-Anderson, A., "Will Weather Dampen Self-Driving Vehicles?" *Bull. Am. Meteorol. Soc.* 101, no. 11 (Nov. 2020): E1914-E1923.

8. "Traffic Safety Facts: Overview: 2008 Data," *PsycEXTRA Dataset*, 2009, doi:10.1037/e626152012-001.

9. Hearst Autos Research, "ADAS: Everything You Need to Know," *Car and Driver*, Apr. 13, 2020, https://www.caranddriver.com/research/a31880412/adas/ (accessed Dec. 17, 2021).

10. Goberville, N.A., Kadav, P., and Asher, Z.D., "Tire Track Identification: A Method for Drivable Region Detection in Conditions of Snow-Occluded Lane Lines," *SAE Int. J. Adv. & Curr. Prac. in Mobility* 4, no. 5 (2022): 1590-1597, https://doi.org/10.4271/2022-01-0083.

11. Kadav, P. and Asher, Z.D., "Improving the Range of Electric Vehicles," in *2019 Electric Vehicles International Conference (EV)*, Oct. 2019, 1-5.

12. Kadav, P., Goberville, N., Motallebiaraghi, F., Fong, A., and Asher, Z.D., "Tire Track Identification: Application of U-Net Deep Learning Model for Drivable Region Detection in Snow Occluded Conditions," in *Intelligent Transportation Systems World Congress*, Los Angeles CA.

13. Sternlund, S., Strandroth, J., Rizzi, M., Lie, A. et al., "The Effectiveness of Lane Departure Warning Systems—A Reduction in Real-World Passenger Car Injury Crashes," *Traffic Inj. Prev.* 18, no. 2 (Feb. 2017): 225-229.

14. Kusano, K.D., Gabler, H., and Gorman, T.I., "Fleetwide Safety Benefits of Production Forward Collision and Lane Departure Warning Systems," *SAE International Journal of Passenger Cars - Mechanical Systems* 7, no. 2 (2014): 514-527, https://doi.org/10.4271/2014-01-0166.

15. Kusano, K.D. and Gabler, H.C., "Comparison of Expected Crash and Injury Reduction from Production Forward Collision and Lane Departure Warning Systems," *Traffic Inj. Prev.* 16, no. Suppl 2 (2015): S109-S114.

16. Gern, A., Moebus, R., and Franke, U., "Vision-Based Lane Recognition under Adverse Weather Conditions Using Optical Flow," *IEEE Intelligent Vehicle Symposium* 2 (Jun. 2002): 652-657.

17. Motallebiaraghi, F. et al., "Mobility Energy Productivity Evaluation of Prediction-based Vehicle Powertrain Control

Combined with Optimal Traffic Management," SAE Technical Paper 2022-01-0141 (2022), https://doi.org/10.4271/2022-01-0141.

18. Zang, S., Ding, M., Smith, D., Tyler, P. et al., "The Impact of Adverse Weather Conditions on Autonomous Vehicles: How Rain, Snow, Fog, and Hail Affect the Performance of a Self-Driving Car," *IEEE Veh. Technol. Mag.* 14, no. 2 (Jun. 2019): 103-111.

19. Rasshofer, R.H., Spies, M., and Spies, H., "Influences of Weather Phenomena on Automotive Laser Radar Systems," *Adv. Radio Sci.* 9 (Jul. 2011): 49-60.

20. "LiDAR," https://www.synopsys.com/glossary/what-is-lidar.html (accessed Oct. 02, 2022).

21. Kulemin, G.P., "Influence of Propagation Effects on a Millimeter-Wave Radar Operation," *Radar Sensor Technology IV* 3704 (Jul. 1999): 170-178.

22. Wallace, H.B., "Millimeter-wave propagation measurements at the Ballistic Research Laboratory," *IEEE Trans. Geosci. Remote Sens.* 26 (May 1988): 253-258.

23. Society of Automotive Engineers, "Taxonomy and Definitions for Terms Related to Driving Automation Systems for On-Road Motor Vehicles," J3016_202104, Apr. 2021.

24. ©Alaska Department of Transportation, P. Facilities, and A. R. Reserved, "[No title]," https://roadweather.alaska.gov/gis (accessed Oct. 05, 2022).

25. "(4) Classification of Road Conditions: From Camera Images and Weather Data," ResearchGate, https://www.researchgate.net/publication/261019430_Classification_of_road_conditions_From_camera_images_and_weather_data (accessed Oct. 05, 2022).

26. Qian, Y., Almazan, E.J., and Elder, J.H., "Evaluating Features and Classifiers for Road Weather Condition Analysis," in *2016 IEEE International Conference on Image Processing (ICIP)*, Sep. 2016, 4403-4407.

27. Kadav, P., Sharma, S., Araghi, F.M., and Asher, Z.D., "Development of Computer Vision Models for Drivable Region Detection in Snow Occluded Lane Lines," in:, *Machine Learning and Optimization Techniques for Automotive Cyber-Physical Systems*, (Springer Nature).

28. "ZED 2 - AI Stereo Camera," https://www.stereolabs.com/zed-2/ (accessed May 10, 2022).

29. Wasserman, S.E. and Monte, D.J., "A Relationship between Snow Accumulation and Snow Intensity as Determined from Visibility," *J. Appl. Meteorol. Climatol.* 11, no. 2 (Mar. 1972): 385-388.

30. "aum-toc.pdf," [Online], available: https://www.weather.gov/media/asos/aum-toc.pdf.

31. Landolt, S.D., Lave, J.S., Jacobson, D., Gaydos, A. et al., "The Impacts of Automation on Present Weather–Type Observing Capabilities across the Conterminous United States," *J. Appl. Meteorol. Climatol.* 58, no. 12 (Dec. 2019): 2699-2715.

32. Martinaitis, S.M., Cocks, S.B., Qi, Y., Kaney, B.T. et al., "Understanding Winter Precipitation Impacts on Automated Gauge Observations within a Real-Time System," *J. Hydrometeorol.* 16, no. 6 (Dec. 2015): 2345-2363.

33. "Snow," https://glossary.ametsoc.org/wiki/Snow (accessed Oct. 13, 2022).

34. Duboue, P., *The Art of Feature Engineering: Essentials for Machine Learning* (Cambridge University Press, 2020)

35. Osisanwo, F.Y., Akinsola, J.E.T., Awodele, O., Hinmikaiye, J.O. et al., "Supervised Machine Learning Algorithms: Classification and Comparison," *International Journal of Computer Trends and Technology (IJCTT)* 48, no. 3 (2017): 128-138.

36. Shetty, S.H., Shetty, S., Singh, C., and Rao, A., "Supervised Machine Learning: Algorithms and Applications," in:, *Fundamentals and Methods of Machine and Deep Learning*, (Wiley, Feb. 24, 2022), 1-16, doi:10.1002/9781119821908.ch1.

37. Motallebiaraghi, F., Rabinowitz, A., and Holden, J., "High-Fidelity Modeling of Light-Duty Vehicle Emission and Fuel Economy Using Deep Neural Networks," SAE Technical, 2021, [Online]. Available: https://www.researchgate.net/profile/Farhang-Motallebiaraghi/publication/350668896_High-Fidelity_Modeling_of_Light-Duty_Vehicle_Emission_and_Fuel_Economy_Using_Deep_Neural_Networks/links/60c9f4aca6fdcc01d476cad8/High-Fidelity-Modeling-of-Light-Duty-Vehicle-Emission-and-Fuel-Economy-Using-Deep-Neural-Networks.pdf

38. Sen, P.C., Hajra, M., and Ghosh, M., "Supervised Classification Algorithms in Machine Learning: A Survey and Review," *Emerging Technology in Modelling and Graphics* (2020): 99-111.

39. Singh, A., Thakur, N., and Sharma, A., "A Review of Supervised Machine Learning Algorithms," in *2016 3rd International Conference on Computing for Sustainable Global Development (INDIACom)*, Mar. 2016, 1310-1315.

40. Pedregosa, V. and Gramfort, "Scikit-Learn: Machine Learning in Python," *Journal of Machine Learning Research*, [Online]. Available:. https://www.jmlr.org/papers/volume12/pedregosa11a/pedregosa11a.pdf?ref=https://githubhelp.com.

41. "Road & Runway Sensors - MARWIS - Mobile Advanced Road Weather Information Sensor," https://www.lufft.com/products/road-runway-sensors-292/marwis-umb-mobile-advanced-road-weather-information-sensor-2308/ (accessed Oct. 13, 2022).

Contact Information

Parth Kadav
Western Michigan University, Kalamazoo, MI 49008 USA
parth.kadav@wmich.edu

Zachary D. Asher, Ph.D.
Western Michigan University, Kalamazoo, MI 49008 USA
zach.asher@wmich.edu

Acknowledgment

Definitions/Abbreviations

ADAS - Advanced Driver Assistance Systems

ASOS - Automated Surface Observing Systems

EEAV - Energy Efficient Autonomous Vehicles Laboratory

LC - Lane-Centering

FCW - Frontal Collision Warning

LDW - Lane Departure Warning

LKA - Lane-Keeping Assist

AEB - Automated Emergency Braking

ODD - Operational Design Domain - domain an autonomous system is designed to operate within

AI/ML - Artificial Intelligence / Machine Learning

CNN - Convolutional Neural Network

DL - Deep Learning

FPS - Frames Per Second

RGB - Red, Green, Blue

MARWIS - Mobile Advanced Road Weather Information Sensor

FARS - Fatality Analysis Report System

Appendix

TABLE 2 All results for the 35 ML model feature set combinations

ML_method	Feature_set	Accuracy	Average Images Computed Per Second	Precision	Recall	IoU	F1_Score
dtrees	0	0.387	4865268	0.387	0.387	0.240	0.387
knn	0	0.459	47328.52	0.459	0.459	0.298	0.459
logistic	0	0.528	23737412	0.528	0.528	0.359	0.528
naive	0	0.528	5954524	0.528	0.528	0.359	0.528
rforest	0	0.434	53057.19	0.434	0.434	0.278	0.434
svm	0	0.528	2729.719	0.528	0.528	0.359	0.528
dtrees	1	0.382	4853586	0.382	0.382	0.236	0.382
knn	1	0.468	48293.94	0.468	0.468	0.305	0.468
logistic	1	0.528	19138612	0.528	0.528	0.359	0.528
naive	1	0.528	6002128	0.528	0.528	0.359	0.528
rforest	1	0.470	56281.48	0.470	0.470	0.307	0.470
svm	1	0.528	2690.322	0.528	0.528	0.359	0.528
dtrees	2	0.377	5070883	0.377	0.377	0.232	0.377
knn	2	0.466	44479.39	0.466	0.466	0.304	0.466
logistic	2	0.528	18959101	0.528	0.528	0.359	0.528
naive	2	0.528	3402475	0.528	0.528	0.359	0.528
rforest	2	0.464	60098.56	0.464	0.464	0.302	0.464
svm	2	0.528	2468.811	0.528	0.528	0.359	0.528
dtrees	3	0.381	4973938	0.381	0.381	0.236	0.381
knn	3	0.462	46111.47	0.462	0.462	0.300	0.462
logistic	3	0.528	22306719	0.528	0.528	0.359	0.528
naive	3	0.528	6158264	0.528	0.528	0.359	0.528
rforest	3	0.461	58234.34	0.461	0.461	0.299	0.461
svm	3	0.528	2701.033	0.528	0.528	0.359	0.528
dtrees	4	0.988	9002163	0.988	0.988	0.975	0.988
knn	4	0.898	45209.99	0.898	0.898	0.814	0.898
logistic	4	0.855	13237942	0.855	0.855	0.746	0.855
naive	4	0.841	5610016	0.841	0.841	0.725	0.841
rforest	4	0.989	91570.39	0.989	0.989	0.978	0.989
svm	4	0.861	6712.247	0.861	0.861	0.755	0.861
dtrees	5	0.988	9513872	0.988	0.988	0.975	0.988
knn	5	0.915	43620.82	0.915	0.915	0.844	0.915
logistic	5	0.837	10435788	0.837	0.837	0.720	0.837
naive	5	0.837	4001418	0.837	0.837	0.720	0.837
rforest	5	0.988	86083.72	0.988	0.988	0.977	0.988
svm	5	0.861	6126.979	0.861	0.861	0.755	0.861

Positions and opinions advanced in this work are those of the author(s) and not necessarily those of SAE International. Responsibility for the content of the work lies solely with the author(s).